A Critical Component of Meiotic Drive in *Neurospora* Is Located Near a Chromosome Rearrangement

Austin M. Harvey,* David G. Rehard,† Katie M. Groskreutz,* Danielle R. Kuntz,* Kevin J. Sharp,* Patrick K. T. Shiu,† and Thomas M. Hammond*,[1]

*School of Biological Sciences, Illinois State University, Normal, Illinois 61790, and †Division of Biological Sciences, University of Missouri, Columbia, Missouri 65211

ABSTRACT *Neurospora* fungi harbor a group of meiotic drive elements known as *Spore killers* (*Sk*). *Spore killer-2* (*Sk-2*) and *Spore killer-3* (*Sk-3*) are two *Sk* elements that map to a region of suppressed recombination. Although this recombination block is limited to crosses between *Sk* and *Sk*-sensitive (Sk^S) strains, its existence has hindered *Sk* characterization. Here we report the circumvention of this obstacle by combining a classical genetic screen with next-generation sequencing technology and three-point crossing assays. This approach has allowed us to identify a novel locus called *rfk-1*, mutation of which disrupts spore killing by *Sk-2*. We have mapped *rfk-1* to a 45-kb region near the right border of the *Sk-2* element, a location that also harbors an 11-kb insertion ($Sk\text{-}2^{INS1}$) and part of a >220-kb inversion ($Sk\text{-}2^{INV1}$). These are the first two chromosome rearrangements to be formally identified in a *Neurospora Sk* element, providing evidence that they are at least partially responsible for *Sk*-based recombination suppression. Additionally, the proximity of these chromosome rearrangements to *rfk-1* (a critical component of the spore-killing mechanism) suggests that they have played a key role in the evolution of meiotic drive in *Neurospora*.

GENOMES typically consist of large groups of cooperating genes that encode information needed to maintain and reproduce themselves as well as their cellular environments. However, individual genes within genomes do not always cooperate (Dawkins 2006; Burt and Trivers 2008). For example, *ranGAP* in fruit flies and *tcd1* in mice are selfish genes that collude with others to bias meiotic transmission ratios to their advantage (Kusano *et al.* 2003; Lyon 2003). While *ranGAP* works within a gene complex known as *Segregation Distorter*, *tcd1* works within another called the *t* haplotype. Because these selfish gene complexes "drive" through meiosis, they are referred to as meiotic drive elements. Such elements are found throughout sexual organisms, with other well-known examples being X^d in stalk-eyed flies, *Ab10* in maize, and the *Spore killers* in various fungi (Rhoades 1942; Raju 1994; Presgraves *et al.* 1997; Burt and Trivers 2008).

Neurospora fungi spend most of their life cycle in a vegetative haploid phase. However, specific environmental cues (*e.g.*, nitrogen limitation) can trigger initiation of the sexual cycle, which includes a brief diploid phase that allows meiotic drive to function in this group of fungi. Sexual reproduction in *Neurospora* begins when an asexual spore (conidium) from a male parent donates a nucleus to an immature fruiting body (protoperithecium) of a female parent. Pairs of nuclei, one from each parent, fuse within the meiotic cells (asci) of the fertilized fruiting body (perithecium) to form a diploid nucleus that passes through the standard stages of meiosis (Raju 1980). The four haploid meiotic products then undergo a postmeiotic mitosis to produce eight nuclei, each of which is incorporated into an American football-shaped ascospore (Raju 1980). Ascospores darken as they mature due to the accumulation of a dark brown pigment. At maturity, fully pigmented "black" ascospores are shot through a small pore at the top of the perithecium. As a result, ascospores typically accumulate on

doi: 10.1534/genetics.114.167007
Manuscript received April 10, 2014; accepted for publication June 7, 2014; published Early Online June 13, 2014.
Supporting information is available online at http://www.genetics.org/lookup/suppl/doi:10.1534/genetics.114.167007/-/DC1.
Sequence data from this article have been deposited with the GenBank accession no. KJ908288.
[1]Corresponding author: 250 Science Laboratory Bldg., School of Biological Sciences, Illinois State University, Normal, IL 61790. E-mail: tmhammo@ilstu.edu

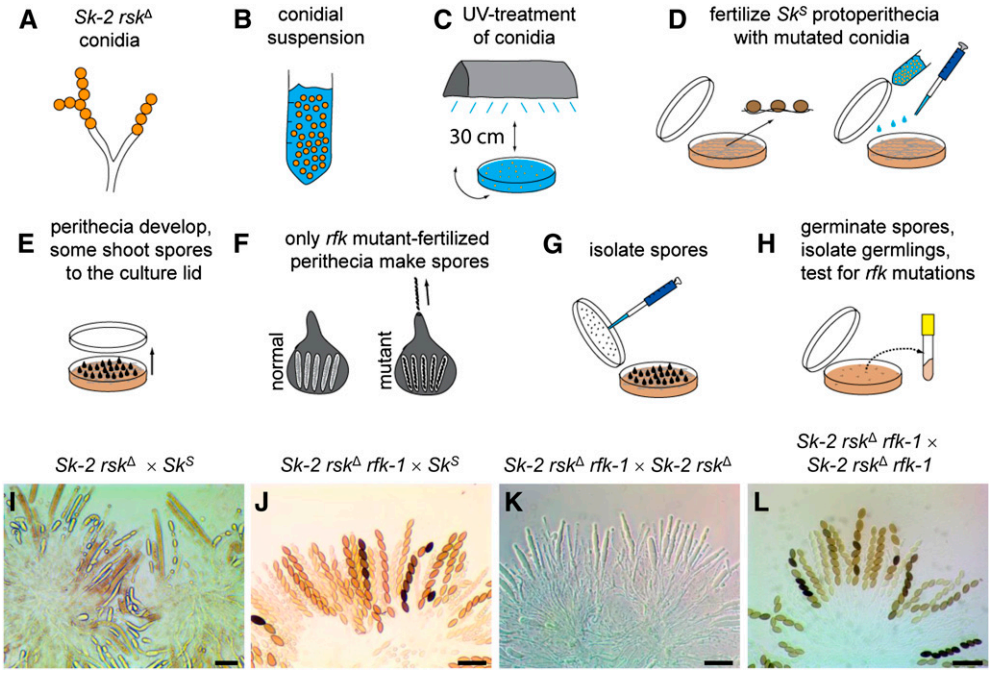

Figure 1 A genetic screen for *rfk* mutations. (A and B) A conidial suspension was made from an *Sk-2 rsk*$^{\Delta}$ strain. (C) The suspension was placed on a 2D rocker under a germicidal lamp and exposed to UV light. (D) The UV-irradiated conidial suspension was used to fertilize a single 6-day-old culture of an *Sk*^{S} strain. The arrow points to a depiction of protoperithecia from the *Sk*^{S} strain. (E and F) Perithecia were allowed to develop for 4 weeks. Theoretically, only perithecia that were fertilized by an *rfk* mutant conidium could produce and shoot viable ascospores. (G and H) Ascospores were isolated and germinated on sorbose medium. Germinating ascospores were selected and transferred to VMM medium in 16-mm test tubes. These cultures were then screened for *rfk* mutations. (I) Asci fail to develop ascospores when *Sk-2 rsk*$^{\Delta}$ (P15-57) is crossed with *Sk*^{S} (F2-26). (J) Ascospore development is normal when *Sk-2 rsk*$^{\Delta}$ *rfk-1* (ISU 3211) is crossed with *Sk*^{S} (F2-23). (K) Asci fail to develop ascospores when *Sk-2 rsk*$^{\Delta}$ *rfk-1* (ISU 3211) is crossed with *Sk-2 rsk*$^{\Delta}$ (ISU 3217). (L) Ascospore development is normal when *Sk-2 rsk*$^{\Delta}$ *rfk-1* (ISU 3211) is crossed with *Sk-2 rsk*$^{\Delta}$ *rfk-1* (ISU 3214). Note that asci develop asynchronously in *N. crassa*. The ascospores with various shades of brown color in I–L have survived spore killing but were still developing when the perithecia were dissected and their asci were imaged. Bars, 60 μm.

the underside of a lid covering an experimental cross when one is made in a standard petri dish.

The three known *Neurospora Spore killers* (*Sk*) are *Sk-1*, *Sk-2*, and *Sk-3*. While *Sk-1* was discovered in *Neurospora sitophila*, *Sk-2* and *Sk-3* were discovered in *N. intermedia* (Turner and Perkins 1979). When a strain harboring one of these *Sk* elements is crossed with a *Spore killer*-sensitive (*Sk*^{S}) strain, many early aspects of sexual reproduction occur as normal (Raju 1979). Indeed, the process that results in killing does not manifest until sometime after the asci start to develop (Raju 1979; Hammond *et al.* 2012b). As a consequence of spore killing, asci will produce four ascospores that are black and viable and four ascospores that are unpigmented and inviable (Turner and Perkins 1979). For simplicity, the unpigmented and inviable ascospores are referred to as white ascospores. The black ascospores are nearly always of the *Sk* genotype (99.9%) (Turner and Perkins 1979), demonstrating that *Sk*-based meiotic drive is very efficient.

Although *Spore killers* have yet to be discovered in other *Neurospora* species, resistance to spore killing (*Sk*^{R}) can be found in wild isolates of the laboratory workhorse *N. crassa* (Turner and Perkins 1979; Turner 2001). This suggests that *N. crassa* populations have harbored *Sk* elements in the past or, alternately, current populations harbor *Sk* elements at such low levels that they have remained undetected. Despite the lack of a naturally occurring *N. crassa Sk* strain to study, much of what we know about the *Sk* elements has been derived from *N. crassa*-based research. This is because Turner and Perkins (1979) introgressed *Sk-2* and *Sk-3* into *N. crassa* shortly after the elements were discovered. This introgression has allowed for *Sk-2* and *Sk-3* to be mapped to chromosome III. However, precise mapping of key loci within the elements has not been possible because they are both associated with a 30-cM region of suppressed recombination. Interestingly, recombination suppression is detected in *Sk* × *Sk*^{S} crosses but it is not detected in *Sk-2* and *Sk-3* homozygous crosses (Campbell and Turner 1987). The reasons for this are unclear. Previously proposed hypotheses include the involvement of *rec* genes, which can affect recombination rates, and/or chromosome rearrangements such as inversions (Campbell and Turner 1987).

Sk-2 and *Sk-3* are considered to be distinct elements even though both are associated with similar regions of chromosome III. The strongest evidence for this is seen in the outcome of *Sk-2* × *Sk-3* crosses, which produce asci with eight white ascospores (Turner and Perkins 1979). It seems these elements both encode unique agents of spore killing and neither *Sk-2* nor *Sk-3* can survive the other's agent. Herein, we refer to these agents as killers.

We recently identified a gene called *rsk* that confers resistance to spore killing (Hammond *et al.* 2012b). *rsk* identification was made possible by a naturally occurring *Sk*^{R} strain of *N. crassa* from Louisiana. Because recombination occurs freely in crosses between *Sk*^{R} and *Sk*^{S} strains (Turner and Perkins 1979), we were able to use two recently

generated *Neurospora* resources—the wild-type (Sk^S) reference genome (Galagan *et al.* 2003) and the *Neurospora* knockout collection (Colot *et al.* 2006)—to map and identify this gene of central importance for the spore killer phenotype (Hammond *et al.* 2012b). Characterization of the *rsk* alleles in Sk^R, *Sk-2*, and *Sk-3* revealed that they all rely on *rsk* to survive meiosis in the presence of a killer. Still, the exact mechanism of *rsk*-mediated resistance is not known. Its elucidation may first require identifying the killer from *Sk-2* and/or *Sk-3*.

Fortunately, there is a feature of *rsk* that could help in this endeavor. For example, when an *Sk-2* strain is deleted of *rsk* and subsequently crossed to an Sk^S strain, meiosis fails and neither black nor white ascospores are produced (Figure 1) (Hammond *et al.* 2012b). The lack of ascospores in *Sk-2* $rsk^{\Delta} \times Sk^S$ crosses suggests that they could be adapted for use in a genetic screen. For instance, one could simply mutate conidia (asexual spores) from an *Sk-2* rsk^{Δ} strain and use the mutant conidia to fertilize protoperithecia of an Sk^S strain. Only fertilization events involving an *Sk-2* rsk^{Δ} conidium that carries a mutation in a gene required for spore killing should produce ascospores.

In this work, we have successfully used this approach to identify a *required for killing* locus (*rfk-1*). Since recombination is suppressed in $Sk \times Sk^S$ crosses, we determined the approximate location of *rfk-1* with mapping experiments conducted solely in the *Sk-2* genetic background. Our results indicate that *rfk-1* is found near the right border of the *Sk-2* element, a region that also holds *Sk-2*-specific chromosome rearrangements.

Materials and Methods

Strains, media, nomenclature, and standard techniques

All strains used in this study are described in Table 1. The mutant alleles used in this study are described in the Neurospora Compendium (Perkins et al. 2000) and e-Compendium (http://www.bioinformatics.leeds.ac.uk/~gen6ar/newgenelist/genes/gene_list.htm). Strain names starting with FGSC were obtained directly from the Fungal Genetics Stock Center (FGSC; McCluskey *et al.* 2010). Vogel's minimal medium (VMM) (Vogel 1956) was used for standard growth and manipulation of *N. crassa* and *N. intermedia* cultures. Bottom agar (BA) and top agar (TA) were used for transformation. For BA, the sucrose in VMM was replaced by a mixture of sorbose, glucose, fructose, and inositol (w/v: 2% sorbose, 0.05% glucose, 0.05% fructose, 0.02% inositol) and 1.5% agar was added. TA was equivalent to BA except that it also contained sorbitol at a concentration of 1 M and only 1% agar was added. Vegetative cultures were incubated at 28° or room temperature. Westergaard and Mitchell's synthetic crossing medium (SCM) was used for sexual crosses (Westergaard and Mitchell 1947), which were performed at room temperature on a laboratory benchtop. Sorbose medium, as described by Brockman and De Serres (1963), was used to isolate progeny from germinating ascospores and to screen mapping populations for leucine auxotrophy and hygromycin resistance. When necessary, media were supplemented with leucine at 4 mM and hygromycin at 200 μg/ml, unless otherwise indicated.

Table 1 Strains used in this study

Strain	Genotype
P6-07[a]	*rid A*
P15-57[a]	*rid*; *Sk-2* rsk^{Δ}::*hph* ; *mus-51*$^{\Delta}$::*bar A*
F2-19[a]	*rid*; *fl*; *Sk-2 A*
F2-23[a]	*rid*; *fl A*
F2-26[a]	*rid*; *fl a*
FGSC 3192	*N. intermedia Sk-2 A*
FGSC 3416	*N. intermedia* Sk^S*A*
FGSC 11245	*ncu06265*$^{\Delta}$::*hph A*
ISU 3199	*rid*; *Sk-2 leu-1*; *mus-51*$^{\Delta}$::*bar a*
ISU 3211	*rid*; *Sk-2* rsk^{Δ}::*hph rfk-1*; *mus-51*$^{\Delta}$::*bar a*
ISU 3212	*rid*; *Sk-2* rsk^{Δ}::*hph rfk-1 a*
ISU 3213	*rid*; *Sk-2* rsk^{Δ}::*hph rfk-1 a*
ISU 3214	*rid*; *Sk-2* rsk^{Δ}::*hph rfk-1*; *mus-51*$^{\Delta}$::*bar A*
ISU 3215	*rid*; *Sk-2* rsk^{Δ}::*hph rfk-1 a*
ISU 3216	*rid*; *Sk-2* rsk^{Δ}::*hph rfk-1 a*
ISU 3217	*rid*; *Sk-2* rsk^{Δ}::*hph A*
ISU 3218	*rid*; *Sk-2* rsk^{Δ}::*hph*; *mus-51*$^{\Delta}$::*bar a*
ISU 3219	*rid*; *fl*; *Sk-2*; *sad-2*$^{\Delta}$::*hph A*
ISU 3221	*rid*; *Sk-2 rfk-1 A*
ISU 3222	*rid*; *Sk-2 rfk-1*; *mus-51*$^{\Delta}$::*bar a*
ISU 3223	*Sk-2 leu-1*; *mus-51*$^{\Delta}$::*bar A*

Throughout this report, when it is necessary to distinguish between an allele in *Sk-2* and an allele in Sk^S, a superscript is added to the end of the gene name. An example is *ncu07880*$^{Sk\text{-}2}$, which refers to the *Sk-2* allele of gene *ncu07880*.

[a] These strains were previously described by Hammond *et al.* (2012b). All strains are available upon request. FGSC strains can also be obtained from the Fungal Genetics Stock Center (McCluskey *et al.* 2010).

Genomic DNA isolation was performed with the DNeasy Plant Mini Kit (QIAGEN, Valencia, CA) or the Genomic DNA Mini Kit for Plants (IBI Scientific, Peosta, IA). DNA amplification via polymerase chain reaction (PCR) or inverse PCR (iPCR) was performed with either an Expand Long Range Polymerase Kit (Roche, Basel, Switzerland) or a Phusion High-Fidelity PCR Kit (New England Biolabs, Ipswich, MA). Additional techniques required for the basic care and handling of *Neurospora* were performed as described by Davis and De Serres (1970).

Isolation of rfk-1

As described in the Introduction, ascospores are not produced in *Sk-2* $rsk^{\Delta} \times Sk^S$ crosses (except for low-level killer escapees, see *Results*). We used this characteristic of *Sk-2* rsk^{Δ} strains to screen for mutants that had lost the ascus-abortion phenotype. The mutagenesis procedure was adapted from Bennett (1979). Specifically, conidia from an *Sk-2* rsk^{Δ} strain (P15-57) were suspended in ice-cold sterile water, filtered with a 100-μm Steriflip filter (EMD Millipore, Billerica, MA), and then diluted to 50 million conidia per milliliter (Figure 1, A and B). A 15-ml aliquot of the conidial suspension was then poured into a 100-mm petri dish on top of a two-dimensional (2D) rocker, which was

Table 2 Phenotypes of the *rfk* mutants isolated in this study

Strain	× *Sk*^{S} (F2-23 or F2-26)	× *Sk-2 rsk*$^\Delta$ (ISU 3217 or ISU 3218)	× *Sk-2 rsk*$^\Delta$ *rfk-1* (ISU 3214)
ISU 3211	Eight black	Ascus abortion	Eight black
ISU 3212	Eight black	Ascus abortion	Eight black
ISU 3213	Eight black	Ascus abortion	Eight black
ISU 3214	Eight black	Ascus abortion	—
ISU 3215	Eight black	Ascus abortion	Eight black
ISU 3216	Eight black	Ascus abortion	Eight black

Six *Sk-2 rsk*$^\Delta$ *rfk-1* mutants were isolated in this study. Each produces normal asci with eight black ascospores when crossed with an *Sk*^{S} strain (column 2), aborted asci when crossed with an *Sk-2 rsk*$^\Delta$ strain (column 3), and normal asci when crossed with another *Sk-2 rsk*$^\Delta$ *rfk-1* strain (column 4).

Table 3 Assembly statistics for the genome of an *N. crassa Sk-2* strain

Statistic	Value
No. sequences[a]	59,497,377
Coverage (fold)	104.9
Contigs	126,508
Average contig length (bp)	341
N50 contig length (bp)[b]	59,983
Max contig length (bp)	426,066
Assembly size (Mb)	43.2

Genomic DNA from strain F2-19 was sequenced with Illumina technology and a draft genome was produced with a *de novo* assembler (see *Materials and Methods*).

[a] Nearly 60 million sequencing reads were used in the assembly.

[b] This value indicates that half of the bases in the assembly are found within contigs of ≥60.0 kb.

used to mix the conidial suspension during UV exposure. The rocker was placed ~30 cm from a G30T8 germicidal lamp (GE, Fairfield, CT) inside a biosafety cabinet. Next, the lid was removed from the petri dish, the rocker was started, and the UV light was turned on for 6 min (Figure 1C). [A viability assay later determined that this process killed ~99.9% of conidia (data not shown).] A 1-ml suspension of the UV-irradiated conidia (50 million conidia) was then used to fertilize a single 6-day-old culture of an *Sk*^{S} strain (F2-26), which was grown on SCM in a 100-mm petri dish (Figure 1D). The fertilized culture was stored in the dark at room temperature for 1 day followed by a 4-week incubation at room temperature on a benchtop. Only a single cross in a single petri dish was performed for this mutagenesis experiment. During incubation of this cross, some of the perithecia produced ascospores that were shot to the lid of the petri dish (Figure 1, E and F). The ascospores were collected, shocked at 60° for 30 min, germinated on sorbose medium, and transferred to individual VMM slants (Figure 1, G and H). The isolates were then screened for resistance to hygromycin and their meiotic phenotypes were determined in crosses with (1) *Sk*^{S}, (2) *Sk-2 rsk*$^\Delta$, and (3) each other.

Sequencing and de novo assembly of the Sk-2 genome

Genomic DNA from an *Sk-2* strain (F2-19) was sent to the University of Missouri-Columbia DNA Core where it was sequenced with Illumina technology. Specifically, an Illumina library preparation kit was used to produce two genomic DNA libraries. Each library was then subject to paired-end sequencing on an Illumina GAII instrument. The unfiltered raw sequences have been deposited in the Sequence Read Archive (Leinonen *et al.* 2011) under accession nos. SRX509482 and SRX510639. The SRX509482 data set has an average insert size of 343 bases and a targeted read length of 120 bases, and the SRX510639 data set has an average insert size of 265 bases and a targeted read length of 80 bases. Quality trimming was performed on the raw sequences by eliminating all bases after the first low-quality base, which was defined as a Phred score <20. Velvet version 1.0.17 (Zerbino and Birney 2008) was used for *de novo* assembly of the sequences.

Mapping contigs from the de novo assembly to the Sk^S *reference genome*

The *N. crassa* reference genome belongs to an *Sk*^{S} strain known as FGSC 2489, a standard laboratory strain (Galagan *et al.* 2003). Version 12 of this reference genome was downloaded from the *Neurospora* Database, which is generously maintained by the Broad Institute of Harvard University and Massachusetts Institute of Technology. Contigs from the *de novo* assembly were mapped to the *Sk*^{S} genome with Nucmer [Nucleotide MUMmer, version 3.07 (Delcher *et al.* 2003)]. Standard PCR assays were then performed to confirm the order of contigs that mapped near the right border of the *Sk-2* element (defined below). If this failed, iPCR was used to determine linkages between select contigs. [iPCR is a technique that can be used to determine the sequence for DNA flanking a known DNA sequence (Dalby *et al.* 1995).] Our iPCR experiments were conducted by digesting 50 ng of *Sk-2* genomic DNA with a restriction enzyme, heat inactivating the enzyme, ligating the restricted ends, and performing PCR with inverted primers. PCR products were then cloned and analyzed by Sanger sequencing.

Miscellaneous computer-based methods

Bioedit [version 7.1.3.0 (Hall 1999)] was used for standard sequence analysis, CLUSTAL W (Thompson *et al.* 1994) was used for pairwise alignments, and BLAST (Altschul *et al.* 1990) was used to search the *Neurospora* Database.

rfk-1 mapping

Our *rfk-1* mapping strategy is similar to that described for *rsk* in Hammond *et al.* (2012a) except the mapping populations were phenotyped for leucine auxotrophy (*leu-1*), resistance to hygromycin (*hph*), and the inability to kill ascospores (*rfk-1*). In each mapping cross, the *hph* markers served as the variable point, while *leu-1* and *rfk-1* served as the anchored points. Before we could begin, the *rsk*$^\Delta$::*hph* allele had to be removed from the genetic background of at least one of the original *rfk-1* strains. This was achieved

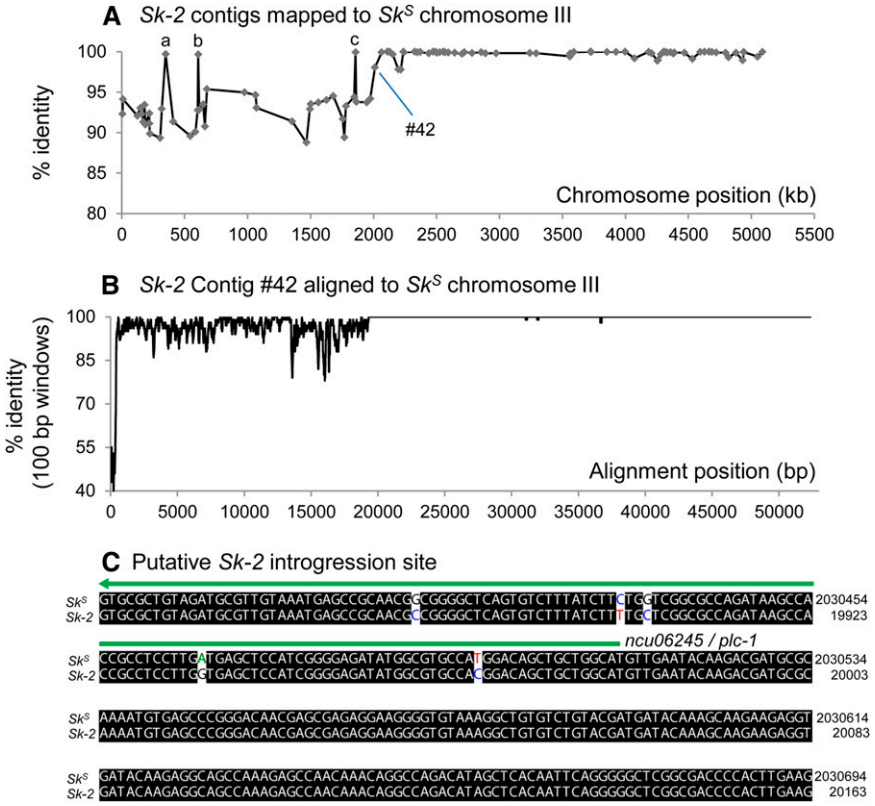

Figure 2 Mapping and analysis of contigs from the draft *Sk-2* genome. (A) Contigs from the *de novo* assembly were mapped to the Sk^S genome (Table S2). The 104 contigs that aligned to Sk^S chromosome III with >50% of their bases and with an alignment >5 kb long were plotted according to their percentage of identity to Sk^S (*y*-axis) and their leftmost mapping position (*x*-axis). A transition from low-identity contigs to high-identity contigs occurs at contig 42. The contigs labeled with lowercase letters (a, b, c) have rightmost mapping positions to the right of contig 42, suggesting they are part of undiscovered chromosome rearrangements or they are partially misassembled. (B) Contig 42 aligns to positions 2,010,595–2,063,714 of Sk^S chromosome III. The scatter plot represents the number of identical nucleotides within 100-bp windows to the right of each aligned position. The aligned sequences were degapped for the identity calculations. (C) The sequence alignment in B becomes nearly identical to that of Sk^S after $ncu06425^{Sk\text{-}2}$.

by crossing an *Sk-2* rsk^{Δ} *rfk-1* strain (ISU 3211) with an *Sk-2* $sad\text{-}2^{\Delta}$ strain (ISU 3219) to obtain *Sk-2 rfk-1* progeny (ISU 3221 and ISU 3222). Mapping populations were then created by crossing strains ISU 3221 or ISU 3222 with various *Sk-2 leu-1 hph* strains (described below).

To create the *hph* marker strains hph^{A} through hph^{G}, an *Sk-2 leu-1* strain (ISU 3223) was transformed with seven different *hph*-based insertion vectors. Vectors were made by joining *Sk-2*-specific DNA flanks to both sides of an *hph* selectable marker with double-joint (DJ)-PCR (Carroll *et al.* 1994; Yu *et al.* 2004; Hammond *et al.* 2011). The primers used to construct these vectors are listed in Supporting Information, Table S1. Transformations were performed using a method similar to one described by Margolin *et al.* (1997). Specifically, conidia were harvested in 30 ml of ice-cold 1 M sorbitol, filtered through a 100-μm Steriflip filter (EMD Millipore, Billerica, MA), pelleted by centrifugation at 2000 × *g* and 10° for 13 min, and resuspended to 2.5×10^9 conidia per milliliter in ice-cold 1 M sorbitol. Approximately 500 ng of transformation vector was added to 100 μl of washed conidia, and the suspension was then mixed gently and briefly incubated on ice (3–10 min) before its transfer to a prechilled 0.1-cm gap-width electroporation cuvette. The DNA and conidia mixture was electroporated at 1500 V with an Eporator (Eppendorf, Hamburg, Germany) and resuspended in 800 μl of ice-cold 1 M sorbitol. This suspension was transferred to 4.2 ml of VMM in a 50-ml conical tube in which it was cultured at 80 rpm and 28° for 3.5 hr. Aliquots of the culture were then suspended in 1 vol of molten TA with a temperature of ~48°. The suspension was then poured onto 2 vol of solidified BA containing 300 μg of hygromycin per milliliter of medium. Culture plates were incubated at 28° for 3–5 days. Transformants were then transferred to VMM slants containing 200 μg of hygromycin per milliliter of medium. Homokaryotic strains were isolated by crossing the hygromycin-resistant transformants to strain F2-26 and isolating progeny derived from hygromycin-resistant ascospores.

To create the hph^{H} marker strain, FGSC 11245 ($ncu06265^{\Delta}$::*hph*) was crossed with ISU 3199 (*Sk-2 leu-1*) and the progeny were screened for spore killing, leucine auxotrophy, and hygromycin resistance. FGSC 11245 is an Sk^S strain from the *Neurospora* knockout collection (Colot *et al.* 2006).

Results

rfk-1 is a locus required for spore killing

Our screen for *rfk* mutants isolated 53 hygromycin-resistant strains. Because the recombination suppression observed in *Sk-2* × Sk^S crosses should lock the rsk^{Δ}::*hph* allele within the *Sk-2* element, hygromycin resistance in these putative *rfk-1* mutants suggested that they are all of the *Sk-2* rsk^{Δ} genotype. We thus examined all 53 strains for loss of the ascus-abortion phenotype associated with *Sk-2* rsk^{Δ} by crossing them with an Sk^S strain. Most of them demonstrated the

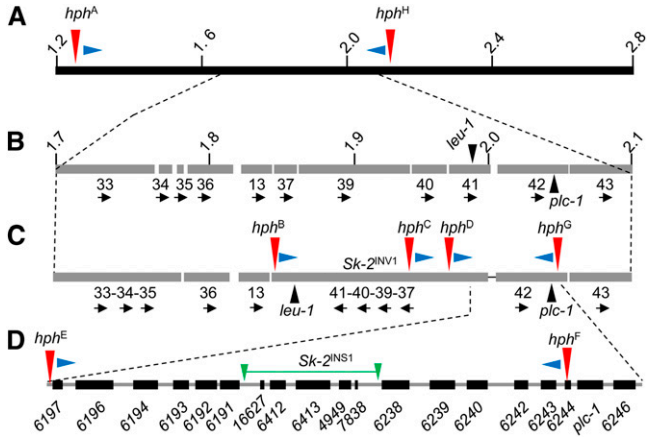

Figure 3 *rfk-1* maps near chromosome rearrangements on the right arm of chromosome III. (A) Hygromycin resistance markers *hph*^{A} and *hph*^{H} were used in three-point crosses with *leu-1* and *rfk-1* (see *Materials and Methods*). The blue arrowheads indicate the direction of *rfk-1* according to the results of the three-point crosses (Table 4). (B) The mapping positions of contigs relative to the *Sk*^{S} reference sequence are shown. Note that contig 13 has a leftmost mapping position at 318 kb. It was included in the diagram because it has a rightmost mapping position at 1845 kb. Attempts to connect it to contigs 36 and 37 were unsuccessful (data not shown). (C) PCR and iPCR assays were used to join several contigs and identify an inversion (*Sk-2*^{INV1}) and an 11-kb insertion (*Sk-2*^{INS1}). (D) A map of *Sk-2*^{INS1} and the surrounding region is shown. Black boxes represent the locations of predicted genes. Gene numbers are listed below the boxes. (C and D) Three-point crosses with *hph* markers (*hph*^{B}–*hph*^{G}) indicate that *rfk-1* should lie within the 45 kb between markers *hph*^{E} and *hph*^{F}.

ascus-abortion phenotype. It is possible that these were derived from ascospores that had escaped spore killing, which is not too surprising since nonresistant ascospores have been observed to do so at a rate of 0.1% (Turner and Perkins 1979). However, we also identified 6 strains that did not demonstrate the ascus-abortion phenotype. These 6 produced normal-looking asci with a full complement of eight black ascospores per ascus (Figure 1J and Table 2, second column), suggesting that each must carry a mutation in an *rfk* gene. Interestingly, ascus abortion returned when we crossed these putative *rfk* mutants to an *Sk-2 rsk*$^{\Delta}$ strain (Figure 1K and Table 2, third column). This suggests that none of the mutants carries a dominant suppressor of spore killing. Finally, the ascus-abortion phenotype was not restored when we crossed the *rfk* mutants to one another (Figure 1L and Table 2, fourth column), suggesting that they are all mutated at the same locus. We thus gave the mutation in each strain the same name: *rfk-1*, for *required for killing-1*.

Sequencing and assembly of the genome from an Sk-2 strain

To help identify the location of *rfk-1*, we sequenced the entire genetic content of an *Sk-2* strain and used a *de novo* assembler to produce a draft of its genome. The assembly used 59,497,377 of 63,637,983 quality-trimmed sequences and contains 126,508 contigs. Although the longest contig in the assembly is just over 426 kb and half of the assembly is found in contigs >60.0 kb, the majority of contigs are <500 bp long. The total size of the assembly is 43.2 Mb, which is <1% longer than the current estimate of 41.7 Mb for the *N. crassa Sk*^{S} reference genome. A summary of these and additional assembly statistics is provided in Table 3.

To simplify analysis of the assembly, we restricted our focus to contigs that aligned to *Sk*^{S} chromosome III with at least 50% of their bases and with a minimum alignment length of 5 kb. We found 104 contigs that fit these criteria (Table S2). Interestingly, the identity of these contigs relative to *Sk*^{S} ranges between 88 and 96% for contigs that align toward the left end of chromosome III, while those that align toward the right end of chromosome III are closer to 100% (Figure 2A and Table S2). Contig 42 appears to be the transition point between these different levels of identity, suggesting it may contain the *Sk-2* introgression site (see below).

To determine the approximate location of *rfk-1*, we randomly chose one of the six *rfk-1* mutants (ISU 3211) for mapping. We then placed a hygromycin marker (*hph*^{A}) between genes *ncu07880*$^{Sk-2}$ and *ncu07881*$^{Sk-2}$ within the *Sk-2* element and used it in a three-point cross with *rfk-1* and *leu-1* (see *Materials and Methods*). The location of *hph*^{A} is equivalent to position 1.22 Mb in the *Sk*^{S} reference genome and the results of the three-point cross indicate *rfk-1* can be found to the right of this position (Figure 3A, Table 4). We then performed a second three-point cross with an *hph* marker located at position 2.12 Mb in the *Sk*^{S} reference genome (*hph*^{H}). Its use in a three-point cross placed *rfk-1* to its left (Figure 3A, Table 4). Together, these data suggest *rfk-1* should lie within *Sk-2* contigs that map between positions 1.22 and 2.12 Mb of the *Sk*^{S} reference genome. This encouraged us to pursue a more detailed analysis of this region within the *Sk-2* element.

The Sk-2 introgression site

As mentioned above, contig 42 appears to be the transition point between contigs with different identity levels to *Sk*^{S} chromosome III. It was thus analyzed more closely for possible evidence of the *Sk-2* introgression site. Figure 2B is a scatter plot showing the percentage of identity of nucleotides within 100-bp windows along an alignment between contig 42 and *Sk*^{S} chromosome III. This analysis reveals that a distinct drop in polymorphisms occurs a little over one-third of the way through the alignment. Specifically, this transition occurs at the 5′ end of a gene called *plc-1*, which encodes phospholipase C (Figure 2C). This location may thus mark the site of *Sk-2*'s introgression from *N. intermedia* into *N. crassa*. If so, the sequences key to *Sk-2*-based meiotic drive must be to its left (*i.e.*, centromere proximal).

Sk-2-specific chromosome rearrangements exist near the introgression site

As part of our characterization of the region between *hph*^{A} and *hph*^{H} in the *Sk-2* element, we attempted to link together

Table 4 Three-point crosses

Marker	Parental genotypes		Interval 1 crossovers		Interval 2 crossovers		Double crossovers		Total
	Crosses predicting the following order: *hph*, *leu-1*, *rfk-1*								
	hph leu-1 +	+ + *rfk-1*	*hph leu-1 rfk-1*	+ + +	*hph* + *rfk-1*	+ *leu-1* +	*hph* + +	+ *leu-1 rfk-1*	
hph^{A}	81	65	2	5	14	11	0	0	178
hph^{B}	171	211	4	8	8	6	0	0	408
	Crosses predicting the following order: *leu-1*, *hph*, *rfk-1*								
	leu-1 hph +	+ + *rfk-1*	*leu-1 hph rfk-1*	+ + +	*leu-1* + *rfk-1*	+ *hph* +	*leu-1* + +	+ *hph rfk-1*	
hph^{C}	204	116	9	8	3	1	1	0	342
hph^{D}	263	239	4	3	6	5	2	0	522
hph^{E}	216	213	11	3	9	11	0	1	464
	Crosses predicting the following order: *leu-1*, *rfk-1*, *hph*								
	leu-1 + *hph*	+ *rfk-1* +	*leu-1* + +	+ *rfk-1 hph*	*leu-1 rfk-1* +	+ + *hph*	*leu-1 rfk-1 hph*	+ + +	
hph^{F}	72	60	1	2	1	2	0	0	138
hph^{G}	125	112	2	4	7	13	0	0	263
hph^{H}	104	156	2	4	7	3	0	1	277

Eight three-point crosses were performed by crossing *Sk-2 leu-1 hph* strains (*hph*^{A}–*hph*^{H}) with *Sk-2 rfk-1* strains (ISU 3221 or ISU 3222). The approximate locations of the *hph* markers are depicted in Figure 3. A "+" is used to indicate normal phenotypes, including leucine prototrophy, hygromycin susceptibility, and the ability to kill ascospores.

contigs that mapped to this area through standard PCR assays. This approach joined contigs 33, 34, and 35, as well as contigs 37, 39, 40, and 41 (Figure 3, B and C; Table 5). We then used a combination of iPCR and Sanger sequencing to discover linkages between some of the remaining unlinked contigs. Unexpectedly, this revealed that contigs 37 and 42 were linked by a chromosome insertion and an inversion (Figure 3, B and C; Table 5). We named these chromosome rearrangements *Sk-2*^{INS1} and *Sk-2*^{INV1} for the insertion and inversion, respectively.

Sk-2^{INS1} is slightly >11 kb long and encodes at least five genes or pseudogenes (Figure 3D and Table 6), which are found at three different locations in the *Sk*^{S} reference genome. For simplicity, we refer to all five sequences as genes. Three of the genes, namely *ncu16627*$^{Sk-2}$, *ncu06412*$^{Sk-2}$, and *ncu06413*$^{Sk-2}$, exist near 1.31 Mb on chromosome III of the *Sk*^{S} reference genome. It thus seems possible they moved to *Sk-2*^{INS1} in a single event. It is also possible all three still encode functional proteins, although *ncu16627*$^{Sk-2}$ has an early stop codon (data not shown). A fourth gene, *ncu07838*$^{Sk-2}$, is normally found near position 1.04 Mb on chromosome III of the *Sk*^{S} genome (Table 6). This gene is lacking >300 bases from its 3′ end, encodes a mutated start codon, and has several early stop codons relative to the allele in *Sk*^{S} (data not shown). Additionally, 28 of 38 detected polymorphisms are thymines in the *Sk-2* allele and cytosines in the *Sk*^{S} allele (Table 6), suggesting that *ncu07838*$^{Sk-2}$ may have been mutated by repeat-induced point mutation (RIP) (Galagan and Selker 2004). A fifth gene, *ncu04949*$^{Sk-2}$, is normally found at 0.84 Mb on chromosome IV of the *Sk*^{S} genome. This gene shows significant signs of RIP, with 95 of the 120 polymorphisms being thymines in the *Sk-2* allele and cytosines in the *Sk*^{S} allele (Table 6). The *Sk-2* allele also encodes many early stop codons (data not shown).

Sk-2^{INS1} is found between genes *ncu06191*$^{Sk-2}$ and *ncu06238*$^{Sk-2}$ of the *Sk-2* element. The former gene is normally at position 1.85 Mb on chromosome III of the *Sk*^{S} genome, but in the *Sk-2* element it is found within inversion *Sk-2*^{INV1} as the most proximal gene to *Sk-2*^{INS1} (Figure 3D). The *Sk-2* contigs thus far linked to *Sk-2*^{INV1} have a total length of 220 kb (Figure 3C, Table 5). We have also identified 47 putative genes within the contigs of *Sk-2*^{INV1} (Table S3). However, since the centromere-proximal end of *Sk-2*^{INV1} is currently undefined, the true length of the inversion must be >220 kb and it likely encodes more than the current estimate of 47 genes.

Because *Sk-2* was introgressed into *N. crassa* from *N. intermedia*, it was conceivable that both *Sk-2*^{INS1} and *Sk-2*^{INV1} could represent the normal arrangement of DNA sequences in *N. intermedia*. To test this, we designed PCR assays to search for the rearrangements in both *N. crassa* and *N. intermedia* strains. Our data indicate that *Sk-2*^{INS1} and *Sk-2*^{INV1} are found in *Sk-2* strains of both species but not in *Sk*^{S} strains of either species (Figure 4). In other words, the chromosome rearrangements are specific to *Sk-2*, not to *N. intermedia*.

The rfk-1 locus maps to a 45-kb region of Sk-2

To better define the location of *rfk-1* between markers *hph*^{A} and *hph*^{H}, six additional *hph* markers (*hph*^{B}–*hph*^{G}) were used in three-point crosses with *leu-1* and *rfk-1* (Figure 3, C and D). These experiments placed *rfk-1* within a 45-kb region of the *Sk-2* element demarcated by markers *hph*^{E} and *hph*^{F} (Figure 3D and Table 4).

Discussion

Meiotic drive elements are widespread among sexual organisms (Burt and Trivers 2008). This may be an unavoidable

Table 5 List of contigs that were tested for contiguity by PCR and iPCR

Contig no.	Length of contig	% identity with *Sk*^{S}	Leftmost mapping position	Rightmost mapping position	Connects to contig
33	28,546	94.5	1,680.2	1,755.6	34
34	12,672	91.7	1,755.7	1,768.4	33, 35
35	14,697	89.4	1,768.4	5,050.2	ND
36	47,063	93.3	1,780.6	1,817.7	ND
13	48,658	92.9	318.0[a]	1,845.2	ND
37	16,926	94.4	1,846.6	3,217.1[a]	42, 39
39	84,516	93.8	1,863.2	1,946.9	37, 40
40	25,999	93.7	1,947.6	1,973.7	39, 41
41	33,400	94.2	1,973.7	2,005.6	40
42	53,528	98.0	2,011.1	2,063.7	37
43	47,339	99.9	2,063.8	2,110.9	ND

Eleven contigs that mapped close to the putative *Sk-2* introgression site (near *plc-1*) were analyzed for contiguity by PCR and iPCR in an effort to better define this region of the *Sk-2* element. The connections discovered through this approach are indicated in the last column. Connections were not discovered (ND) for some contigs.

[a] Note that the leftmost and rightmost mapping positions are not always consistent with the hypothesis that these contigs map near the *Sk-2* introgression site. This may be due to undiscovered chromosome rearrangements or errors during *de novo* assembly.

consequence of sexual reproduction, which places alleles of genes in direct competition with one another for transmission. As a result, alleles that evolve driving mechanisms gain an immediate advantage over their competitors, whether or not that allele is advantageous for the organism as a whole. Although meiotic drive elements are ubiquitous in animals, plants, and fungi, few have been fully characterized at the molecular level. We recently took a significant step forward in elucidating the molecular mechanism of meiotic drive in *Neurospora* fungi when we identified *rsk*, a gene required for *resistance to spore killing* (Hammond *et al.* 2012b). Here, by eliminating *rsk* from an *Sk-2* strain, it became possible for us to screen for mutations in genes that are *required for killing* (*rfk*), leading to the discovery of *rfk-1*.

How many *rfk* loci are there? Thus far it appears that *rfk-1* may be the only locus required for killing. For example, our mutant screen identified six *rfk* mutants, all of which failed to complement each other's inability to kill spores (Table 2, right column). The odds of this happening if there are two similarly sized loci required for killing are rather low (1/32). Nevertheless, a couple of reasons prohibit us from ruling out there being more than one *rfk* locus. One is that different *rfk* mutants may be unable to complement spore killing in heterozygous crosses. This would explain why our different *rfk* strains failed to complement one another (Table 2, right column). Another reason is that all six of our mutants were recovered from a single cross made in a single petri dish. This suggests that all of our mutants could have originated from a single perithecium, which could explain why they are all mutated at the same locus. It thus seems that a definitive answer on the number of *rfk* loci (one or more than one) must await further experimentation.

How does the *rfk-1* mutation eliminate killing? There are at least three scenarios that could account for the loss of killing in *rfk-1* mutants. First, *rfk-1* could be a locus that is directly targeted by the killer. In this scenario only the *rfk-1* ascospores should resist killing; however, this is clearly not the case as all ascospores resist killing when *Sk-2 rsk*$^\Delta$ *rfk-1* is crossed with *Sk*^{S} (Figure 1J and Table 2, second column). A second possibility is that *rfk-1* encodes a mutant protein that directly suppresses the killer. This seems unlikely because the ascus-abortion phenotype is observed in crosses between *Sk-2 rsk*$^\Delta$ *rfk-1* and *Sk-2 rsk*$^\Delta$ (Figure 1K and Table 2, third column), suggesting that the latter strain's killer is functional even when *rfk-1* is present. Finally, *rfk-1* may encode the killer itself or it may encode a protein that synthesizes the killer. This is the simplest explanation and it would account for all of our results. This explanation is also consistent with the "killer-neutralization model" (Hammond *et al.* 2012b). This model holds that RSK is present throughout meiosis, where its job is to find and neutralize the killer. Once an ascospore reaches a certain stage of development (*e.g.*, after delimitation), it becomes responsible for producing its own RSK. Therefore, only an ascospore that encodes a resistant version of RSK will survive killing. Assuming RFK is the killer or that it makes the killer, it seems that (i) it must have a long half-life so it can remain inside non-*Sk* ascospores after they become delimited or (ii) it must not be ascospore autonomous, which would allow it to leave the *Sk* ascospores and enter their non-*Sk* siblings after delimitation.

To more efficiently map *rfk-1*, we sequenced the genome of an *Sk-2* strain. Although it may have been possible to design *hph* insertion vectors based on the *Sk*^{S} reference sequence and still conduct our mapping experiments successfully, the presence of chromosome rearrangements could have interfered with this approach. Fortunately, our sequencing and assembly efforts discovered the *Sk-2*-specific chromosome rearrangements *Sk-2*^{INV1} and *Sk-2*^{INS1}, which helped make sense of the gene orders obtained for *hph*, *leu-1*, and *rfk-1* when markers *hph*$^{B–E}$ were used in three-point crossing assays.

Table 6 Analysis of *Sk-2*^{INS1}

Position[a]	Blastx (*E* value)[b]	*Sk*^{S} location[c]	% nucleotide identity (differences)[d]	*Sk*^{S} CG to *Sk-2* TA[e]	*Sk-2* CG to *Sk*^{S} TA[f]
1–1,098	No hits				
1,099–1,444	*ncu16627* (4e-39)	III, 1.32	90.8 (32)	16	1
1,445–1,928	No hits				
1,929–3,280	*ncu06412* (0)	III, 1.31	93.6 (86)	30	17
3,281–4,126	No hits				
4,127–7,057	*ncu06413* (0)	III, 1.31	96.3 (108)	32	32
7,058–7,795	No hits				
7,796–8,824	*ncu04949* (0)	IV, 0.84	88.5 (120)	95	5
8,825–9,153	No hits				
9,154–9,406	*ncu07838* (4e-17)	III, 1.04	85.0 (38)	28	7
9,407–11,034	No hits				

The 11,034-bp *Sk-2*^{INS1} sequence was used to search the *N. crassa* database for matching proteins.

[a] Preliminary searches were performed to help locate gene boundaries, which allowed us to parse the sequence into 11 fragments.

[b] Each fragment was then used as the query sequence in a BLAST search of *N. crassa* proteins, using 1e-3 as the cutoff value for matching sequences. Only the top-scoring match for each search is shown.

[c] The approximate location of the protein in the *Sk*^{S} genome is indicated by chromosome and position in megabases.

[d] CLUSTAL W alignments were performed between the DNA sequences of the genes in *Sk-2* and *Sk*^{S}. These alignments were used to calculate percentage of nucleotide identity. The total number of polymorphic bases is indicated in parentheses. Two of the five genes are truncated in *Sk-2* relative to their alleles in *Sk*^{S}. Specifically, there are 34 bases missing from the 3′ end of *ncu04949*$^{Sk\text{-}2}$ and 310 bases missing from the 3′ end of *ncu07838*$^{Sk\text{-}2}$. The missing bases were not included in the identity calculations.

[e] The total number of positions where the *Sk*^{S} sequence is a cytosine and the *Sk-2* sequence is a thymine plus where the *Sk*^{S} sequence is a guanine and the *Sk-2* sequence is an adenine.

[f] Similar to the previous column except that the strains are reversed.

One unexplained aspect of our mapping data concerns a discrepancy between the numbers of parental genotypes recovered in crosses involving *hph*^{C} (Table 4, 204 and 116) and *hph*^{H} (Table 4, 104 and 156). This suggests there could be undetected phenotypes associated with some of the parental genotypes. For example, ascospore germination rate and colony expansion rate could lead to biases in progeny isolation because progeny were isolated as single ascospore-derived colonies on sorbose medium. Colonies were typically rejected if they were too close to a neighboring colony. It is also possible that some genotypes are less resistant to the heat-shock method used to break ascospore dormancy. In any case, it is unlikely that any potential bias in progeny selection or heat-shock survivability affected the primary finding that *rfk-1* is located between markers *hph*^{E} and *hph*^{F} since all eight crossing experiments are consistent with this hypothesis. Additionally, there appears to be little to no discrepancy in progeny numbers within parental or recombination classes for all other crosses, including the most critical crosses involving *hph*^{E} and *hph*^{F} (Table 4).

With respect to the *Sk-2* and *Sk-3* regions of suppressed recombination (which are sometimes referred to as "recombination blocks"), previous cytological analyses and genetic marker-based studies failed to provide clear evidence for chromosome rearrangements (Campbell and Turner 1987). Our discovery of an inversion near the right border of the *Sk-2* element provides at least a partial explanation for the existence of suppressed recombination. However, assuming that the *Sk-2* element encompasses nearly all of chromosome III up to *ncu06238*$^{Sk\text{-}2}$, and based on the position of *ncu06238* in the *Sk*^{S} reference genome, the *Sk-2* element can be estimated to be ~2 Mb long. With this estimate, the currently defined 220 kb of *Sk-2*^{INV1} represents just 11% of *Sk-2*. Other rearrangements may thus be involved with suppressing recombination throughout the element. It seems incorporating a longer read technology could simplify the task of identifying other inversions and filling the gaps in our current version of the *Sk-2* sequence. For example, many of the contigs in our current assembly end with repetitive sequences (data not shown), possibly explaining why they were not joined to other contigs by the *de novo* assembler. Longer reads could help span such repetitive sequences, possibly allowing many of the current contigs to be joined *in silico* rather than by laborious iPCR assays. Since suppressed recombination is crucial for the survival of a meiotic drive element (because the killer cannot afford to segregate away from its resistance gene), the full characterization of the recombination-suppression mechanism should continue to interest those studying selfish elements.

Acknowledgments

We thank members of our laboratories and our colleagues for their help and support and we are grateful to the anonymous reviewers for their helpful advice on improving the manuscript. We acknowledge use of materials generated by grant P01 GM068087, "Functional Analysis of a Model Filamentous Fungus, from the National Institute of General Medical Sciences." This work was supported by the National Science Foundation (MCB1157942, to P.T.K.S.) and a New Faculty Initiative grant from Illinois State University (to T.M.H.).

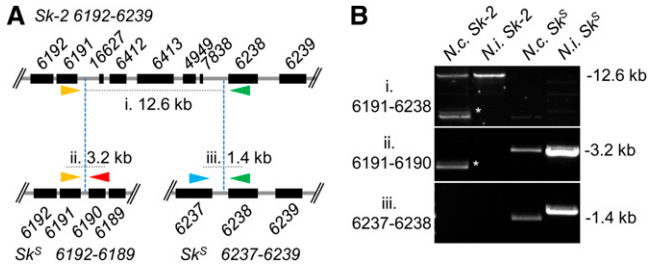

Figure 4 The *Sk-2*^{INV1} and *Sk-2*^{INS1} chromosome rearrangements are not standard features of the *N. intermedia* genome. (A) A diagram of the region spanning the end of *Sk-2*^{INV1} (between genes *ncu06191* and *ncu16627*) and *Sk-2*^{INS1} is depicted above the corresponding regions as they exist in the *N. crassa Sk*^{S} reference strain. The colored arrowheads indicate oligonucleotide primer binding sites and the direction of amplification. We used the following oligonucleotide primers in the PCR assays: green, no. 291 5′ GTTCGCTGACTTTCCCGACCAT 3′; blue, no. 292 5′ GGAGTTGCGGTCTTGGTGTCCTG 3′; orange, no. 293 5′ CGAAGGAGGAGGCGATGGTGTT 3′; and red, no. 294 5′ GGCAGTTGGCTCTGGGATGGA 3′. Predicted product sizes (gray dashed lines) are as follows: i, 12.6 kb; ii, 3.2 kb; and iii, 1.4 kb. (B) PCR assays were used to determine if the *Sk-2* rearrangements are specific to *Sk-2*. (i) A PCR product spanning *Sk-2*^{INS1} was amplified from *N. crassa* and *N. intermedia Sk-2* but not from *N. crassa* and *N. intermedia Sk*^{S}. (ii) A PCR product spanning *ncu06191* and *ncu06190* was detected only in *Sk*^{S} strains, suggesting these genes are no longer linked in *Sk-2* strains. The asterisks in i and ii denote a couple of nonspecific bands that are often amplified from *N. crassa Sk-2* when primer 293 is used in the PCR reaction (data not shown). (iii) A PCR product spanning *ncu06237* and *ncu06238* was also detected only in *Sk*^{S} strains, suggesting these genes are also no longer linked in *Sk-2* strains. Strains: *N.c. Sk-2*, F2-19; *N.i. Sk-2*, FGSC 3192; *N.c. Sk*^{S}, P6-07; *N.i. Sk*^{S}, FGSC 3416.

Literature Cited

Altschul, S. F., W. Gish, W. Miller, E. W. Myers, and D. J. Lipman, 1990 Basic local alignment search tool. J. Mol. Biol. 215: 403–410.

Bennett, J. W., 1979 Aflatoxins and anthraquinones from diploids of *Aspergillus parasiticus*. J. Gen. Microbiol. 113: 127–136.

Brockman, H. E., and F. J. de Serres, 1963 Sorbose toxicity in *Neurospora*. Am. J. Bot. 50: 709–714.

Burt, A., and R. Trivers, 2008 *Genes in Conflict: The Biology of Selfish Genetic Elements*. Harvard University Press, Cambridge, MA.

Campbell, J. L., and B. C. Turner, 1987 Recombination block in the *Spore killer* region of *Neurospora*. Genome 29: 129–135.

Carroll, A. M., J. A. Sweigard, and B. Valent, 1994 Improved vectors for selecting resistance to hygromycin. Fungal Genet. Newsl. 41: 22.

Colot, H. V., G. Park, G. E. Turner, C. Ringelberg, C. M. Crew *et al.*, 2006 A high-throughput gene knockout procedure for *Neurospora* reveals functions for multiple transcription factors. Proc. Natl. Acad. Sci. USA 103: 10352–10357.

Dalby, B., A. J. Pereira, and L. S. Goldstein, 1995 An inverse PCR screen for the detection of P element insertions in cloned genomic intervals in *Drosophila melanogaster*. Genetics 139: 757–766.

Davis, R. H., and F. J. de Serres, 1970 Genetic and microbiological research techniques for *Neurospora crassa*. Methods Enzymol. 17: 79–143.

Dawkins, R., 2006 *The Selfish Gene: 30th Anniversary Edition*. Oxford University Press, London/New York/Oxford.

Delcher, A. L., S. L. Salzberg, and A. M. Phillippy, 2003 Using MUMmer to identify similar regions in large sequence sets. Curr. Protoc. Bioinformatics Chap. 10: Unit 10.3.

Galagan, J. E., and E. U. Selker, 2004 RIP: the evolutionary cost of genome defense. Trends Genet. 20: 417–423.

Galagan, J. E., S. E. Calvo, K. A. Borkovich, E. U. Selker, N. D. Read *et al.*, 2003 The genome sequence of the filamentous fungus *Neurospora crassa*. Nature 422: 859–868.

Hall, T. A., 1999 BioEdit: a user-friendly biological sequence alignment editor and analysis program for Windows 95/98/NT. Nucleic Acid Symp. Ser. 41: 95–98.

Hammond, T. M., H. Xiao, D. G. Rehard, E. C. Boone, T. D. Perdue *et al.*, 2011 Fluorescent and bimolecular-fluorescent protein tagging of genes at their native loci in *Neurospora crassa* using specialized double-joint PCR plasmids. Fungal Genet. Biol. 48: 866–873.

Hammond, T. M., D. G. Rehard, B. C. Harris, and P. K. T. Shiu, 2012a Fine-scale mapping in *Neurospora crassa* by using genome-wide knockout strains. Mycologia 104: 321–323.

Hammond, T. M., D. G. Rehard, H. Xiao, and P. K. T. Shiu, 2012b Molecular dissection of *Neurospora Spore killer* meiotic drive elements. Proc. Natl. Acad. Sci. USA 109: 12093–12098.

Kusano, A., C. Staber, H. Y. Chan, and B. Ganetzky, 2003 Closing the (Ran)GAP on segregation distortion in *Drosophila*. BioEssays 25: 108–115.

Leinonen, R., H. Sugawara, and M. Shumway, 2011 The sequence read archive. Nucleic Acids Res. 39: D19–D21.

Lyon, M. F., 2003 Transmission ratio distortion in mice. Annu. Rev. Genet. 37: 393–408.

Margolin, B. S., M. Freitag, and E. U. Selker, 1997 Improved plasmids for gene targeting at the *his-3* locus of *Neurospora crassa* by electroporation. Fungal Genet. Newsl. 44: 34–36.

McCluskey, K., A. Wiest, and M. Plamann, 2010 The Fungal Genetics Stock Center: a repository for 50 years of fungal genetics research. J. Biosci. 35: 119–126.

Perkins, D. D., A. Radford, and M. S. Sachs, 2000 *The Neurospora Compendium: Chromosomal Loci*. Academic Press, Waltham, MA.

Presgraves, D. C., E. Severance, and G. S. Willrinson, 1997 Sex chromosome meiotic drive in stalk-eyed flies. Genetics 147: 1169–1180.

Raju, N. B., 1979 Cytogenetic behavior of spore killer genes in *Neurospora*. Genetics 93: 607–623.

Raju, N. B., 1980 Meiosis and ascospore genesis in *Neurospora*. Eur. J. Cell Biol. 23: 208–223.

Raju, N. B., 1994 Ascomycete spore killers: chromosomal elements that distort genetic ratios among the products of meiosis. Mycologia 86: 461–473.

Rhoades, M. M., 1942 Preferential segregation in maize. Genetics 27: 395–407.

Thompson, J. D., D. G. Higgins, and T. J. Gibson, 1994 CLUSTAL W: improving the sensitivity of progressive multiple sequence alignment through sequence weighting, position-specific gap penalties and weight matrix choice. Nucleic Acids Res. 22: 4673–4680.

Turner, B. C., 2001 Geographic distribution of *Neurospora* spore killer strains and strains resistant to killing. Fungal Genet. Biol. 32: 93–104.

Turner, B. C., and D. D. Perkins, 1979 *Spore killer*, a chromosomal factor in *Neurospora* that kills meiotic products not containing it. Genetics 93: 587–606.

Vogel, H. J., 1956 A convenient growth medium for *Neurospora* (Medium N). Microb. Genet. Bull. 13: 42–43.

Westergaard, M., and H. K. Mitchell, 1947 *Neurospora* V. A synthetic medium favoring sexual reproduction. Am. J. Bot. 34: 573–577.

Yu, J. H., Z. Hamari, K. H. Han, J. A. Seo, Y. Reyes-Domínguez *et al.*, 2004 Double-joint PCR: a PCR-based molecular tool for gene manipulations in filamentous fungi. Fungal Genet. Biol. 41: 973–981.

Zerbino, D. R., and E. Birney, 2008 Velvet: algorithms for *de novo* short read assembly using de Bruijn graphs. Genome Res. 18: 821–829.

Communicating editor: D. A. Barbash

GENETICS

Supporting Information
http://www.genetics.org/lookup/suppl/doi:10.1534/genetics.114.167007/-/DC1

A Critical Component of Meiotic Drive in *Neurospora* Is Located Near a Chromosome Rearrangement

Austin M. Harvey, David G. Rehard, Katie M. Groskreutz, Danielle R. Kuntz, Kevin J. Sharp, Patrick K. T. Shiu, and Thomas M. Hammond

DOI: 10.1534/genetics.114.167007

Table S1 Oligonucleotide primers used to construct *hph* vectors

hph[A]	insertion between *ncu07880*$^{Sk\text{-}2}$ and *ncu07881*$^{Sk\text{-}2}$
199-A	5' CCACGACGACCAAACACAAGACC 3'
199-B	5' ATGCTCCTTCAATATCAGTTGCTTCGCTTCCAACGTCCCTCT 3'
199-C	5' ATGCCGACCGGGAACCAGTTCGTTCACCTTCACGAGACCCTCA 3'
199-D	5' GCTGACCCAACTGGTCGTCACTC 3'
199-E	5' ATCACCTGGGGCTGGAACTACAC 3'
199-F	5' GCGAGCTTTTTACCCGCGAACC 3'
hph[B]	insertion between *ncu06235*$^{Sk\text{-}2}$ and *ncu06236*$^{Sk\text{-}2}$
222-A	5' CATCTGGTCGCCTTCCAACTGCT 3'
222-B	5' ATGCTCCTTCAATATCAGTTTCCCCTCACTGGTCTCTTCCTTTTG 3'
222-C	5' ATGCCGACCGGGAACCAGTTGCACCCCTGGACGGCTAATG 3'
222-D	5' GCACTTCCGATGCTGAGAGACC 3'
222-E	5' TCACCTGTCGTTTGCGGGTAGAA 3'
222-F	5' GGGCTTGCTTTGCTGGGTTAGGT 3'
hph[C]	insertion between *ncu06227*$^{Sk\text{-}2}$ and *ncu06228*$^{Sk\text{-}2}$
221-A	5' TTGGGCTACCGCCTACCGAAC 3'
221-B	5' ATGCTCCTTCAATATCAGTTGACAAGGGTCTGATTTGATTGACGA 3'
221-C	5' ATGCCGACCGGGAACCAGTTGCCGTCCAGCCACTTGTTTGTC 3'
221-D	5' GCGGATTATTGCTCTGATTGGTAGG 3'
221-E	5' CGGACGCCAACATACACAGTCTCA 3'
221-F	5' TGTCTTGGTCTACCTCACCACCTCA 3'
hph[D]	insertion between *ncu06212*$^{Sk\text{-}2}$ and *ncu06213*$^{Sk\text{-}2}$
242-A	5' TCCTCCTCCTCCTCCTCCTCC 3'
242-B	5' ATGCTCCTTCAATATCAGTTGCAGTTGATGTTCCCTTCTGTGTG 3'
242-C	5' ATGCCGACCGGGAACCAGTTCAGAATTGCTCCAGACAGCACACC 3'
242-D	5' CCGAGATCGCAAACAAGGCTAA 3'
242-E	5' TCCCAACATACCAGCACCACCA 3'
242-F	5' AACTTCAGGAGCAAGGGC 3'
hph[E]	insertion between *ncu06197*$^{Sk\text{-}2}$ and *ncu11314*$^{Sk\text{-}2}$
240-A	5' CTTCCAGCCATCATCAACGACCA 3'
240-B	5' ATGCTCCTTCAATATCAGTTGCACAACGCAACAGGAAACCAAA 3'
240-C	5' ATGCCGACCGGGAACCAGTTACTGGTGGAGGAGAAGGGGACTG 3'
240-D	5' CGAGGTCTCAAGCCGACAATCAA 3'
240-E	5' AGGCCAAAACCCCAAATAGTGAAGG 3'
240-F	5' ATGGACTGGAAAGCATGACGAAAGG 3'
hph[F]	deletion of *ncu06244*$^{Sk\text{-}2}$
225-A	5' GGCGACAGAAAGGGCAAAGGAG 3'
225-B	5' ATGCTCCTTCAATATCAGTTGATGGGGGCAGGGAGAGAGAAA 3'
225-C	5' ATGCCGACCGGGAACCAGTTATTTGGTTGTGGTGGTGGTGGTG 3'
225-D	5' CTGGGACGGGCGGTTATGTTCT 3'
225-E	5' GCGCCCAAGAAGAAGGTGGAAC 3'
225-F	5' GCGCCAAACTTACCGACTCTAATCC 3'
hph[G]	insertion between *ncu06247* and *ncu06248*
223-A	5' GCTTTGTAGGTTGGCGGTGATG 3'
223-B	5' ATGCTCCTTCAATATCAGTTCCCTCCCGTGTGTTCGTGATAGA 3'
223-C	5' ATGCCGACCGGGAACCAGTTCCCGAAGTGCAGATCCAGAAAGA 3'
223-D	5' ACCACGGCAGGGTAGGTGATGAA 3'
223-E	5' GGGAATGGATTGGAAGCGAAGGT 3'
223-F	5' GTCGCCGGGTGGTTGATTTGT 3'

The oligonucleotide primers listed above were used in a double-joint (DJ)-PCR protocol for the construction of *hph*-based transformation vectors (Yu *et al*. 2004; Hammond *et al.* 2011). Primers with names ending with "A" or "B" were used to amplify the left flank of the vectors, "C" or "D" were used for the right flanks, and "E" or "F" were used for nested amplification of the final vector. Primers that were the reverse complement of "C" and "D" were used to amplify the *hph* marker from plasmid pCB1004 or a derivative of pCB1004 (CARROLL *et al.* 1994).

Carroll, A. M., J. A. Sweigard, and B. Valent, 1994 Improved vectors for selecting resistance to hygromycin. Fungal Genet. Newsl. 41: 22.

Hammond, T. M., H. Xiao, D. G. Rehard, E. C. Boone, T. D. Perdue et al., 2011 Fluorescent and bimolecular-fluorescent protein tagging of genes at their native loci in *Neurospora crassa* using specialized double-joint PCR plasmids. Fungal Genet. Biol. 48: 866–873.

Yu, J. H., Z. Hamari, K. H. Han, J. A. Seo, Y. Reyes-Domínguez et al., 2004 Double-joint PCR: a PCR-based molecular tool for gene manipulations in filamentous fungi. Fungal Genet. Biol. 41: 973–981.

Table S2 *Sk-2* contigs

Contig #	length	% ident.	leftmost position (kb)	rightmost position (kb)		Contig #	length	% ident.	leftmost position (kb)	rightmost position (kb)
1	13768	92.3	6.5	516.8		53	20446	100.0	2372.0	2391.8
2	94042	94.1	9.1	124.1		54	31630	99.8	2438.3	2469.7
3	19299	92.1	124.1	403.7		55	19920	100.0	2472.0	2492.2
4	14469	93.0	147.7	1107.8		56	9350	100.0	2492.4	2501.5
5	59060	92.3	158.7	503.8		57	24575	99.9	2501.8	2526.0
6	38896	91.3	171.4	217.9		58	26545	99.9	2526.2	2552.6
7	187692	93.4	181.0	1295.3		59	14202	100.0	2553.8	2567.9
8	32186	91.0	187.8	1310.7		60	26245	99.9	2567.9	2594.0
9	118483	92.4	219.4	5062.8		61	72909	99.9	2594.1	2645.5
10	44274	91.1	219.9	967.8		62	56043	99.9	2645.5	2701.1
11	21193	89.9	224.1	974.7		63	19862	99.7	2701.1	2720.5
12	16832	89.4	305.2	4281.9		64	63243	100.0	2720.5	2783.0
13	48658	92.9	318.0	1845.2		65	73408	99.9	2783.0	2855.1
14	18444	99.7	348.5	4579.1		66	34061	99.9	2855.3	2888.9
15	69302	91.4	409.6	1680.1		67	80721	99.8	2889.4	2969.0
16	36605	89.6	544.8	584.4		68	94241	99.8	2974.3	3067.6
17	33117	90.1	585.0	615.7		69	54046	99.8	3239.9	3291.5
18	94731	92.8	603.4	1466.6		70	262331	99.8	3291.7	3552.5
19	32795	99.7	607.4	2424.2		71	29922	99.4	3559.1	4560.7
20	33337	92.8	615.7	647.1		72	30066	99.8	3560.1	3589.8
21	16220	93.5	647.1	663.5		73	134022	100.0	3589.8	3722.5
22	13612	90.8	660.7	676.2		74	5719	100.0	3722.9	3728.5
23	9057	95.4	676.3	683.2		75	126370	100.0	3728.8	3853.6
24	105421	95.0	975.0	2010.4		76	72411	100.0	3853.6	3925.3
25	12455	94.7	1062.7	5049.1		77	73677	100.0	3925.4	3998.7
26	28690	93.1	1071.1	1093.5		78	44288	100.0	3998.7	4042.9
27	28977	91.4	1353.7	4862.9		79	113473	99.2	4072.7	4183.5
28	9414	88.8	1466.6	1475.7		80	24629	100.0	4183.7	4207.5
29	7293	92.9	1493.8	1500.9		81	48813	99.8	4207.5	5214.9
30	36760	93.5	1502.1	1537.1		82	63582	98.9	4255.5	5272.3
31	82243	93.7	1562.8	1624.0		83	62672	99.0	4257.8	5212.6
32	12208	94.0	1626.5	1638.8		84	21046	99.7	4281.5	5170.9
33	28546	94.5	1680.2	1755.6		85	13256	100.0	4302.5	4315.4
34	12672	91.7	1755.7	1768.4		86	18113	100.0	4315.4	4333.3
35	14697	89.4	1768.4	5050.2		87	24561	99.9	4333.6	4358.1
36	47063	93.3	1780.6	1817.7		88	24148	99.9	4358.2	4382.4
37	16926	94.4	1846.6	3217.1		89	49616	99.8	4382.4	4444.6
38	174465	99.9	1856.7	3239.9		90	34866	99.9	4387.2	4468.0
39	84516	93.8	1863.2	1946.9		91	60919	99.9	4468.3	4529.0
40	25999	93.7	1947.6	1973.7		92	9015	99.1	4531.8	5046.5
41	33400	94.2	1973.7	2005.6		93	32097	100.0	4594.9	4626.9
42	53528	98.0	2011.1	2063.7		94	36473	100.0	4626.9	4663.3
43	47339	99.9	2063.8	2110.9		95	24196	100.0	4663.6	4687.5
44	15069	100.0	2110.9	2126.0		96	48811	100.0	4687.8	4720.8
45	27896	100.0	2126.0	2153.4		97	74480	99.9	4721.0	4794.4
46	44311	99.7	2153.4	2196.6		98	24115	99.9	4794.4	4818.7
47	20267	97.8	2196.8	2439.1		99	60854	99.3	4818.7	4879.2
48	12962	97.8	2217.0	2229.8		100	28680	99.9	4879.2	4907.2
49	5306	100.0	2236.8	2242.0		101	8061	98.9	4932.0	4939.9
50	123372	99.9	2242.1	2327.0		102	97858	100.0	4939.9	5037.3
51	21070	100.0	2327.0	2347.9		103	27975	99.4	5050.2	5077.9
52	24158	99.9	2348.1	2371.9		104	67266	100.0	5087.3	5153.2

Contigs from the *de novo* genome assembly for an *Sk-2* strain (F2-19) were aligned to version 12 of the *N. crassa* genome (see Materials and Methods). The table contains all contigs that align to chromosome III with more than 50% of their bases and with

an alignment more than 5 kb. We named the contigs according to their leftmost mapping position. Statistics were calculated from the combined local alignments for each contig with custom Perl scripts.

Table S3 Genes found within *Sk-2*^{INV1}

Contig	Gene name		Contig	Gene name
#41	*ncu06236*		#39	*ncu06220*
	ncu06235			*ncu06218*
	ncu06234			*ncu06217*
	ncu06233			*ncu06216*
	ncu06232			*ncu06215*
	ncu06231			*ncu06214*
	ncu06230			*ncu06213*
	ncu06229			*ncu06212*
#40	*ncu06228*			*ncu06211*
	ncu06227			*ncu06210*
	ncu06226			*ncu06209*
	ncu11311			*ncu06207*
	ncu11312			*ncu06206*
	ncu11313			*ncu06205*
	ncu06224			*ncu06204*
	ncu06223			*ncu06203*
	ncu06222			*ncu06202*
	ncu06221			*ncu06201*
#37	*ncu06197*			*ncu06200*
	ncu06196			*ncu16645*
	ncu06194			*ncu06199*
	ncu06193			*ncu06198*
	ncu06192			*ncu11314*
	ncu06191			

Genes located within the *Sk*^{S} regions that aligned with Contigs #37, #39, #40, and #41 were identified by searching the *N. crassa* database. They were then confirmed to exist within *Sk-2* Contigs #37, #39, #40, and #41 with CLUSTAL W alignments. Note that the total number of genes within *Sk-2*^{INV1} is likely to increase once its centromere-proximal end has been defined.